Measuring the Resolving Power of Ion Mobility Spectrometers

ARTICLE *in* ANALYTICAL CHEMISTRY · DECEMBER 1994

Impact Factor: 5.64 · DOI: 10.1021/ac00095a014

6 AUTHORS, INCLUDING:

William Siems
Washington State University
101 PUBLICATIONS **2,852** CITATIONS
SEE PROFILE

Ching Wu
Excellims Corporation
30 PUBLICATIONS **1,112** CITATIONS
SEE PROFILE

Anal. Chem. **1994,** *66,* 4195–4201

Measuring the Resolving Power of Ion Mobility Spectrometers

William F. Siems,* Ching Wu, Edward E. Tarver, and Herbert H. Hill, Jr.

Department of Chemistry, Washington State University, Pullman, Washington 99164-4630

Paul R. Larsen and Dennis G. McMinn

Department of Chemistry, Gonzaga University, Spokane, Washington 99258-0001

Ion mobility spectrometry peak width data are fitted by a least-squares procedure to a semiempirical model having three adjustable parameters. Peaks are wider than contributions from initial pulse width and diffusion predict, and it is suggested that the additional width is due mainly to electric field inhomogeneity and Coulombic repulsion. The effects of operating conditions and instrument dimensions on resolving power are discussed. It is proposed that increased inhomogeneity of the electric field results in lower measured mobility values, as well as lower resolving power.

For ion mobility spectrometry (IMS),[1] as for any separation technique, the ability of an instrument to resolve closely spaced peaks is of considerable interest. While IMS peak shapes have been analyzed[2] and the effects of drift voltage, gate pulse width, temperature, and mobility on resolving power have been studied,[3] the effects of specific instrument design characteristics such as length and diameter of the drift region have been less well characterized. The earlier studies used mathematical models based on idealized conceptions of electric field uniformity and pulse shape, and while there has been good qualitative agreement between the models and experiment, quantitative agreement has been less satisfactory. We have followed and expanded on a suggestion of Revercomb and Mason[4] by fitting measured peak width data against theoretical pulse width and diffusion width variables. The resulting slope and intercept values become empirical parameters in our revised model. The model's predictions correspond well to observed line widths across a wide range of operating conditions, and the parameter values can be related to instrument design characteristics and used to discuss differences between instruments.

The most useful definition of resolving power, R, for IMS is the single-peak-based quotient

$$R = t_d/w \tag{1}$$

where t_d is the drift time of an ion of interest and w is the temporal peak width measured at half-height. The drift time of an ion is related in theory to the length of the drift space in centimeters, L, the voltage drop across the drift space, V, and the mobility of the ion in cm²/Vs, K:

$$t_d = L^2/KV \tag{2}$$

Equation 2 is a rearranged form of the fundamental mobility equation $v_d = KE$, where v_d is the drift velocity in cm/s and E is the electric field strength in V/cm.

The major factors determining IMS peak shape are the initial shape of the bundle of ions admitted to the drift region and the diffusional broadening of the bundle as it travels to the collector. If an initial pulse gated into the drift region were of Gaussian shape with width at half-height t_g, then the peak gathered at the collector would also be Gaussian with width at half-height w and

$$w^2 = t_g^{\,2} + t_{diff}^{\,2} \tag{3}$$

where t_{diff} is the width at half-height of the Gaussian peak that would be produced by diffusional broadening of an infinitely narrow initial pulse. The initial pulse is in fact not Gaussian. In the first place, the gating control is usually generated as a step function. Spangler and Collins[2] achieved close fits of experimental peak shapes by convoluting a step function, representing initial pulse shape, with a Gaussian function representing diffusional broadening. On the other hand, although the voltage applied to a gate can closely approximate a step function, Aronson's mathematical model of gating has shown that ion density across a closed gate drops to zero considerably less rapidly than a step function[5] and that this profile is retained by the leading edge of an ion bundle that is admitted to the drift region when the gate opens. This same study showed that the trailing edge of an ion pulse, created as an open gate suddenly closes, also slopes less abruptly than a step function. Further, the position and slope of the leading and trailing edges were found to depend on the details of the gating (gate closure field, wire diameter, and spacing).

Another imperfection of eq 3 is its neglect of the diffusion that takes place while an ion pulse is being collected, which causes the trailing edges of all ion peaks to be slightly more diffuse than their leading edges. With these caveats about peak shape in mind, we chose eq 3 as the starting point for this study.

(1) For an introduction to ion mobility spectrometry, see: Hill, H. H., Jr.; Siems, W. F.; St. Louis, R. H.; McMinn, D. G. *Anal. Chem.* **1990**, *62*, 1201A–1209A and references listed therein.
(2) Spangler, G. E.; Collins, C. I. *Anal. Chem.* **1975**, *47*, 403–407.
(3) Rokushika, S.; Hatano, H.; Baim, M. A.; Hill, H. H., Jr. *Anal. Chem.* **1975**, *57*, 1902–1907.
(4) Revercomb, H. E.; Mason, E. A. *Anal. Chem.* **1975**, *47*, 970–983.
(5) Aronson, E. A. Technical Report No. SAND87-0072; Sandia Corp.: Albuquerque, NM, 1987.

0003-2700/94/0366-4195$04.50/0

The spatial spreading of an ion peak, arriving at the collector t_d seconds after being admitted to the drift space as an extremely narrow pulse, is governed by its diffusion coefficient, D (in cm^2/s):

$$\sigma_{space} = (2Dt_d)^{1/2} \tag{4}$$

In the low electric field generally employed in IMS, the diffusion coefficient has a simple connection to mobility, expressed in the Einstein relation

$$D = kTK/q \tag{5}$$

where k is the Boltzmann's constant, q is the charge on the ion, and T is the absolute temperature. Inserting eqs 2 and 5 into eq 4 gives

$$\sigma_{space} = \left[\frac{2kT}{qV}\right]^{1/2} L \tag{6}$$

The spatial spreading of the ion pulse is related to the temporal duration measured at the collector by[4]

$$\frac{\sigma_{space}}{L} = \frac{\sigma_{time}}{t_d} \tag{7}$$

Finally, using eq 7 and the usual relation between the standard deviation and peak width at half-height ($t_{diff} = (8 \ln 2)^{1/2}\sigma_{time}$), we arrive at

$$t_{diff} = \left[\frac{16 \ln 2kT}{qV}\right]^{1/2} t_d \tag{8}$$

The resulting model equation for measured peak widths,

$$w^2 = t_g^2 + \frac{16 \ln 2\, k}{q} \frac{Tt_d^2}{V} \tag{9}$$

is equivalent to Spangler and Collins's eq 12 (aside from the Townsend energy factor),[2] Revercomb and Mason's eq 82,[4] and Rokushika et al.'s eq 13 (aside from an extra factor of 2 chosen by those authors for reporting peak widths).[3]

Spangler and Collins[2] measured Cl^- peak widths at 160.3 °C and E = 214 V/cm using initial pulse widths between 0.05 and 1.00 ms. To achieve a good fit between predicted and measured values, they increased the diffusional contribution to peak width by using a modified form of the Einstein relation which included η, the Townsend energy factor:[6]

$$D = \frac{\eta kTK}{q} \tag{10}$$

The Townsend factor takes into account that the ions may be at a higher effective temperature than the drift gas, since the ions are continually receiving energy from the electric field and hence may not be in thermal equilibrium with their surroundings. The best fit between prediction and experiment was obtained by the authors with η = 2.7. However, because η is known to be close to 1 for ions under conditions common in IMS experiments (see ref 6, p 533), such a high value cannot be correct, and there must be another explanation for the additional peak broadening observed.

Rokushika et al. studied resolving power for the $H(H_2O)_n^+$ reactant ion as a function of temperature, electric field, and initial pulse width and resolving power for a series of methyl ester product ions as a function of mobility.[3] While good qualitative agreement with the predictions of eq 9 was obtained, measured values of resolving power were in all cases lower than theoretical by about 33%. In discussing possible reasons for peak widths greater than theoretical predictions, the authors dismissed ion–molecule reactions in the drift space and mutual Coulombic repulsion between like-charged ions. In fact, the earlier work of Spangler and Collins[2] and a recent argument by Spangler[7] have shown that Coulombic repulsion, although less important than diffusional broadening, does contribute measurably to peak widths, and that the effect becomes more pronounced as the initial pulse width increases. Nevertheless, Coulombic broadening cannot account for discrepancies of the magnitude reported by Rokushika et al. It is interesting to note that these are of the same magnitude as those treated earlier by Spangler and Colins with introduction of the η parameter,[2] a result which might be expected given the similarity of the instruments employed in the studies (built by Franklin GNO in one case and its successor, PCP Inc. of West Palm Beach, FL, in the other). Finally, Rokushika et al. suggest without discussion that the discrepancy in peak widths could be due to the difficulty of achieving a smooth electric field throughout the drift region, an idea with which we concur and will discuss further below.

Revercomb and Mason have suggested that gating behavior could be studied by plotting w^2 vs t_d^3 or $1/V^3$ (equivalent since $t_d \propto 1/V$) for a single ion, while keeping t_g constant. If the initial pulse shape were Gaussian, the plot would be a straight line, and deviations from linearity would give information about the initial distribution.[4] Realizing that semiempirical fitting of line width data could help us evaluate the contributions of various physical processes to measured values, we have substituted the following expression for eq 9:

$$w^2 = \gamma + \beta t_g^2 + \alpha \frac{Tt_d^2}{V} \tag{11}$$

Here α, β, and γ are parameters that can be adjusted to give the best fit to parameters t_g, V, and T and the measured values t_d and w. The third term is the "diffusion" contribution to pulse width, although it may include other effects with the same voltage dependence as diffusion (increased effective temperature of the ions or electric field inhomogeneity, for example). A plot of w^2 vs Tt_d^2/V (which we refer to as the diffusion parameter) would have a slope $\alpha = 0.957 \times 10^{-3}$ if eq 9 were obeyed exactly, whereas if other broadening processes are operative, a larger value would be obtained for the slope. The second term is the "gate width" contribution to peak width, although it could include other broadening processes that increase along with increasing gate width (Coulombic repulsion, for example). A plot of w^2 vs t_g^2

(6) McDaniel, E. W. *Collision Phenomena in Ionized Gases*; Wiley: New York, 1964; Chapter 11.

(7) Spangler, G. E. *Anal. Chem.* **1992**, *64*, 1312.

Table 1. Physical Dimensions and Operating Conditions of IMS Instruments

	IMS instrument			
	A	B	C	D
drift region length (cm)	15.6	11.6	7.0	8.0
drift region diam (cm)	4.9	4.9	2.5	4.3
ionization region length (cm)	8.0	8.0	3.0	6.0
ionization region diam (cm)	3.0	3.0	1.5	1.4
ions measd	$(H_2O)_nH^+$, Cl^-	$(H_2O)_nH^+$	O_2^-	$(H_2O)_nH^+$
temp range (°C)	275	175–325	80–90	240
drift voltage range	2118–4941	1871–4366	1120–2800	1143–1600
t_g range (ms)	0.10–0.50	0.10–0.50	0.10–0.30	0.05–0.50

would have a slope $\beta = 1$ if eq 9 were obeyed exactly, while a larger value could be evidence for broadening by Coulombic repulsion. The first term is the "constant" contribution to pulse width, equal to zero in eq 9, but possibly of nonzero value if factors unaffected by gating or voltage are present. Such factors could include instrumental response times and, possibly, dynamic aspects of ion distributions around opening and closing gates.

To obtain an expression related to resolving power, we divide eq 11 by t_d^2:

$$R^{-2} = \frac{\gamma + \beta t_g^2}{t_d^2} + \frac{\alpha T}{V} = R_p^{-2} + R_d^{-2} \qquad (12)$$

where

$$R_p = \frac{t_d}{(\gamma + \beta t_g^2)^{1/2}} = \frac{L^2}{(\gamma + \beta t_g^2)^{1/2} KV} \qquad (13)$$

is the *pulse-width-only resolving power*, the resolving power that would be observed if diffusion were insignificant, and

$$R_d = (V/\alpha T)^{1/2} \qquad (14)$$

is the *diffusion-only resolving power*, the resolving power that would be obtained with zero initial pulse width and $\gamma = 0$. Note that overall resolving power will be dominated by the *smaller* of R_p and R_d.

In undertaking these studies, we wanted to test whether eq 11 would, in fact, be a good model of peak widths; in addition, we wanted to find α, β, and γ values that would be characteristic of particular IMS instruments over a wide range of operating conditions and that could be used to compare the resolving power of instruments. Finally, we wanted to use these values as a basis for discussing aspects of instrument design that influence resolving power.

EXPERIMENTAL SECTION

Measurements were made using four different IMS instruments, the physical dimensions of which are given in Table 1. Tubes A and B were high-temperature prototypes built at Washington State University, using guard rings fashioned from stainless steel shim stock cemented inside alumina tubing. A schematic diagram of tube B is shown in Figure 1. Tube C was a prototype built by Honeywell CDC, Clearwater, FL, using a traditional stacked ring construction. Tube D was a Phemto-Chem

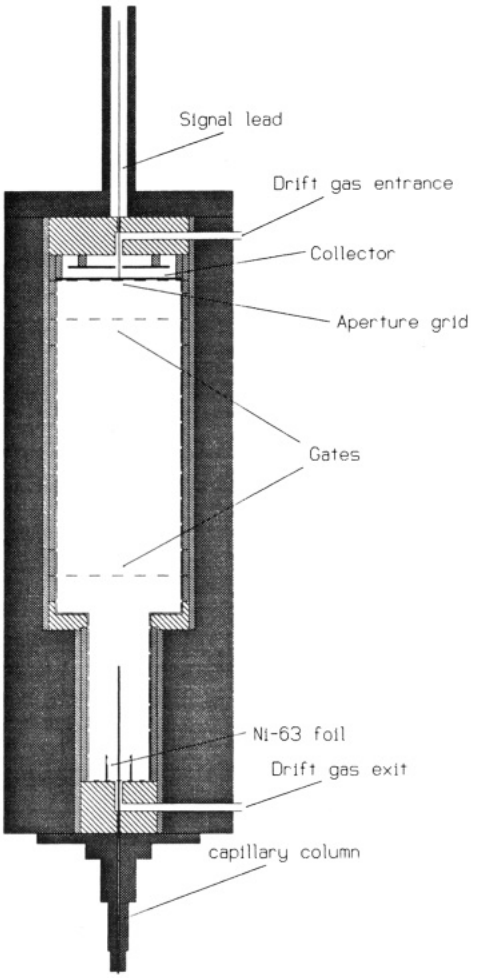

Figure 1. Ion mobility spectrometer.

100 built by PCP Inc. of West Palm Beach, FL, also having a stacked ring design. In all the instruments, guard rings were 0.9 cm wide, separated by 0.1 cm insulators. All used a 10 mCi ^{63}Ni foil as ionization source, except tube A, which used a 25 mCi source. Drift gas flow rate was typically 500 mL/min, and drift tube pressure was typically 700 Torr. Measurements of drift time and peak width were made over ranges of temperature, drift voltage, and initial pulse width for a variety of ions, as summarized in Table 1.

Since the software used with all these instruments has the start of data acquisition coinciding with the rising edge of the gating pulse, drift times were obtained from $t_d = t_{meas} - t_g/2$, where t_{meas} is the time coordinate of the peak maximum. To obtain the most accurate possible measurement of peak widths at half-height, w, from our digitized data, an interpolation procedure was used to locate the time coordinates of the half-height crossings. The data

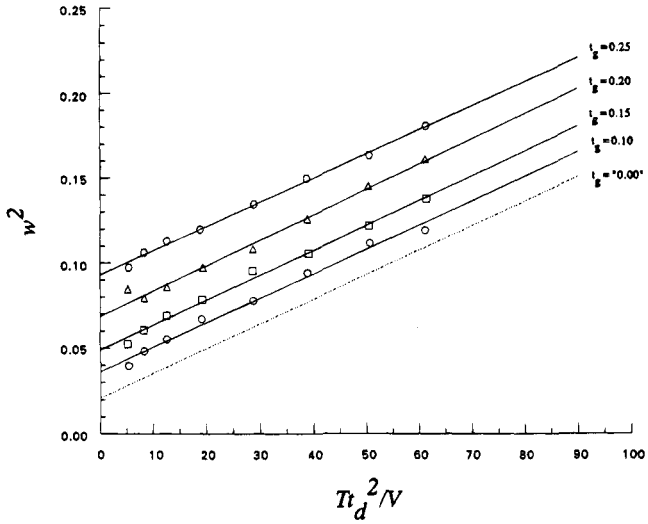

Figure 2. Measured width squared as a function of diffusion parameter for various initial pulse widths. *T*, 275 °C; *L*, 11.6 cm.

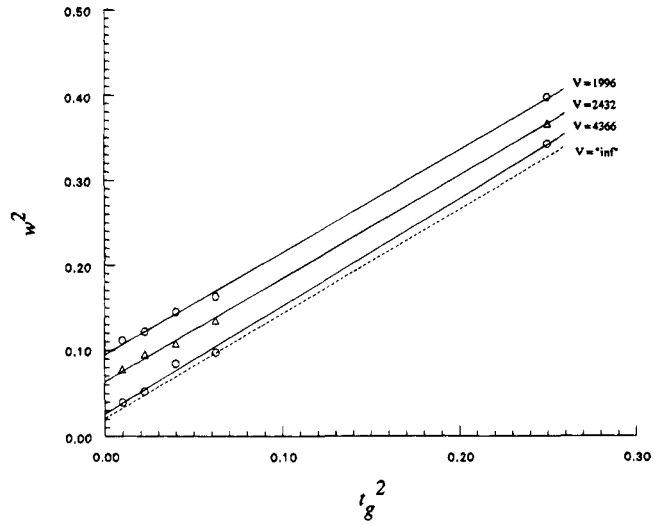

Figure 3. Measured width squared as a function of pulse width squared at various voltages. *T*, 275 °C; *L*, 11.6 cm.

were then subjected to a series of least-squares fitting procedures to determine the α, β, and γ parameters. All the figures to follow pertain to width measurements of the $(H_2O)_nH^+$ reactant ion, although a series of measurements on Cl^-, obtained by chromatographic introduction of CH_2Cl_2 into tube A, was used to confirm that the α, β, and γ parameters for the Cl^- product ion were essentially the same as those for the $(H_2O)_nH^+$ reactant ion. Figure 2 is an example plot of w^2 vs Tt_d^2/V (the slope of which is α), while Figure 3 is an example plot of w^2 vs t_g^2 (the slope of which is β). The solid lines in the two figures show the least-squares fits of the experimental data. In Figure 3, the points at $t_g^2 = 0.25$ are far removed from the other points, have high leverage on the fitted slopes, and thus could raise concerns about the goodness of the linear fit and the values of the slopes. However, other data sets with more evenly spaced points also showed good linearity and similar slope values. The dotted line in Figure 2 was obtained by plotting and performing a least-squares fit of the intercept values of the lines from Figure 3 (thus corresponding to $t_g = 0.00$), while the dotted line in Figure 3 was similarly obtained by plotting and fitting the intercept values of the lines from Figure 2 (corresponding to infinite voltage or zero diffusion). The intercept of the dotted line in either Figure 2 or Figure 3 is an estimate of the γ parameter.

Table 2. Summary of Results from Fitting Peak Width Data

IMS device	$\alpha \times 10^3$ (V/K)	β	$\gamma \times 10^8$ (s^2)	V_{opt}[a]	R_{max}[a]	R_{max}/R_{ideal}[b]
ideal	0.957	1	0	2693	61.4	1
tube A (L = 15.6 cm)	1.40	1.60	0.61	2640	50.2	0.80
tube B (L = 11.6 cm)	1.43	1.24	2.1	1659	39.4	0.80
tube C (L = 7.0 cm)	6.5	1.23	1.5	921	13.8	0.49
tube D (L = 8.0 cm)	1.26	1.13	0.47	1089	34.0	0.88

[a] Calculated for T = 225°C, t_g = 0.20 ms, and K = 4.25 cm^2/Vs. The "ideal" tube is assumed to have a length of 15.6 cm for computing V_{opt} and R_{max}. [b] Calculated for t_g = 0.20 ms.

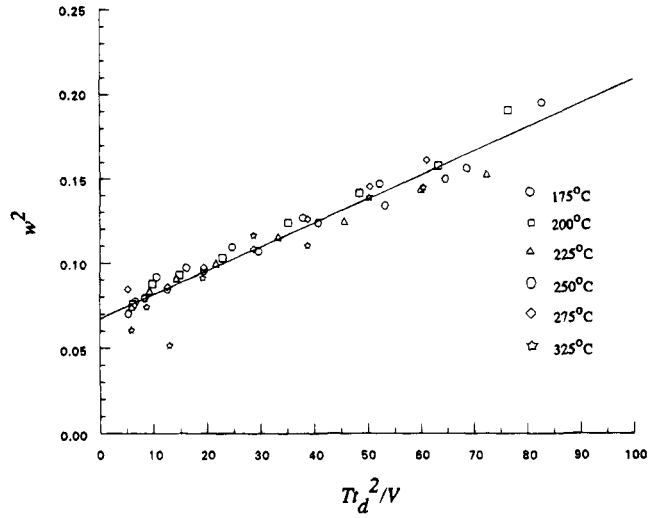

Figure 4. Measured width squared as a function of diffusion parameter at various temperatures. t_g, 0.20 ms; *L*, 11.6 cm.

RESULTS AND DISCUSSION

Quality of the Fit between Model and Experiment. The results of fitting the line width data for the four IMS instruments to eq 11 is summarized in Table 2. The single α, β, and γ parameter values shown in the table for tubes A, C, and D were obtained by averaging all individual values obtained from lines such as those shown in Figures 2 and 3. The data from tube B were treated in an alternate but similar fashion by performing a simultaneous least-squares fit of all experimental data points to eq 11.

The goodness of the fit between eq 11 and experimental width data can be shown with a few example plots. Equation 11 indicates that a plot of w^2 vs Tt_d^2/V for a single t_g and ranging T and V should yield a straight line. Figure 4 shows such a plot for data gathered using tube B, with t_g = 0.20 ms and six temperatures ranging from 175 °C to 325 °C. The solid straight line is a least-squares fit of all the data (slope, 1.41×10^{-3}; intercept, 0.0674). Most of the points lying above the line belong to the lower three temperatures, while most of the points lying below the line belong to the higher three temperatures. The reduced mobility[1] of the $(H_2O)_nH^+$ peak does not change appreciably over the temperature range studied, making it unlikely that changes in cluster size are responsible for the temperature dependence seen in Figure 4. Least-squares fits of data from individual temperature series yield essentially parallel lines. Thus any temperature dependence of

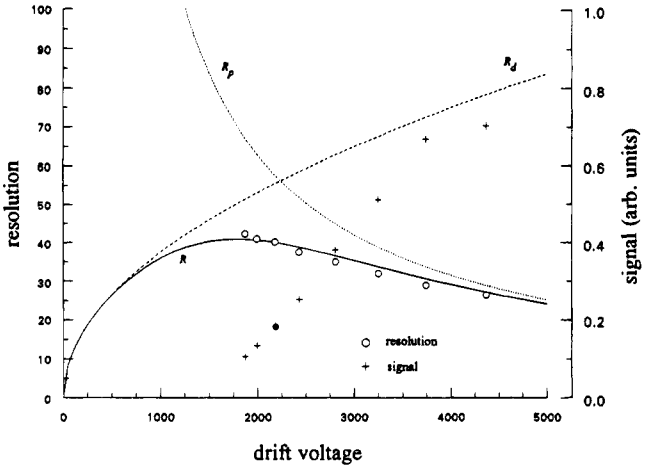

Figure 5. Diffusion and pulse width contributions to resolving power. T, 225 °C; t_g, 0.20 ms; L, 11.6 cm.

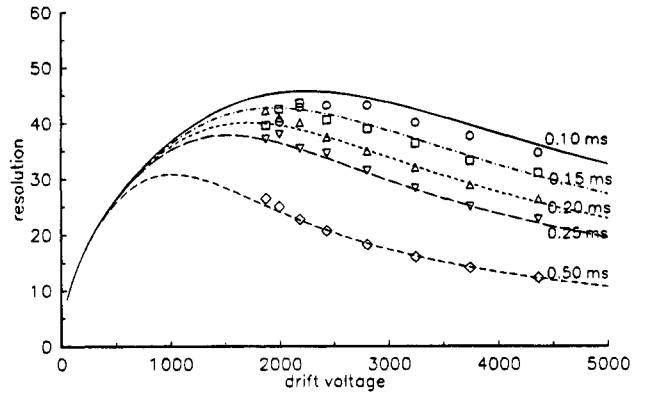

Figure 6. Effect of gate pulse width on resolving power. T, 225 °C; L, 11.6 cm.

α is small. Data for other t_g values show a similar behavior to Figure 4, and all the data taken together are consistent with both β and γ decreasing slightly as temperature increases.

Figure 5 shows measured resolving power values for tube B (T = 225 °C, t_g = 0.20 ms, V ranging) as open circles, together with calculated lines for R, R_p, and R_d as given by eqs 12–14, using the α, β, and γ values from Table 2. At low drift voltage, diffusion is the major factor determining peak width, whereas at high voltage, the initial pulse width becomes dominant. Note how R remains below the R_d and R_p lines, approaching them asymptotically at low and high drift voltage, respectively. Around V = 1500, there is a maximum in the resolving power curve, a situation which will be discussed in the next section. It should be noted that IMS instruments are generally operated at voltages higher than that giving maximum resolving power, as the position of the open circles suggests. The reason for this is that signal levels drop off about linearly with decreasing drift voltage, a manifestation of the usual tradeoff between sensitivity and resolving power. Experimental signal levels are shown as crosses on Figure 5.

Figure 6 shows several sets of measured resolving power values for tube B at T = 225 °C and a range of pulse widths, plus corresponding lines calculated as for Figure 5. The calculated lines do not fit the data for narrow initial pulses as well as they fit the wide pulse data because the least-squares procedure that was used minimizes the magnitude of differences between calculated and experimental widths. A procedure minimizing relative differences would lead to a more uniform-appearing fit. The points in the neighborhood of the maximum resolving power show both

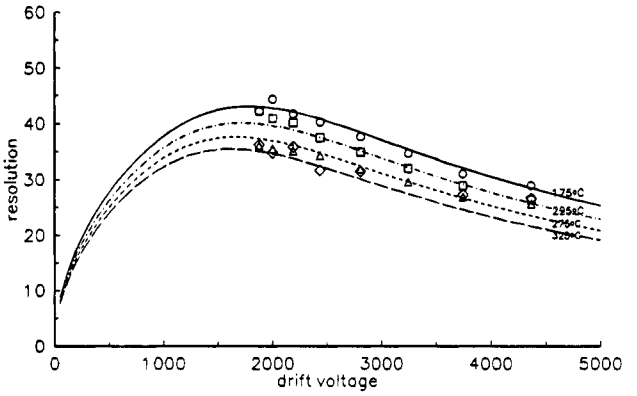

Figure 7. Effect of temperature on resolving power. t_g, 0.20 ms.

Table 3. Functional Dependence of Resolving Power on Operating Parameters

	drift voltage	temp	pulse width	tube length	mobility
$R_d \ll R_p$	$V^{1/2}$	$T^{-1/2}$			
$R_p \ll R_d$	V^{-1}	T^{-1}	t_g^{-1}	L^2	K^{-1}

the most scatter and the least satisfactory correspondence between experimental points and model predictions. From the experimental side, these are the measurements with greatest uncertainty, both because of the high relative uncertainty in measuring the widths of narrow peaks and because the peak intensities are quite low. On the model side, these are the calculated points most affected by small changes in the α, β, and γ parameters.

Figure 7 plots experimental resolving power values for tube B with t_g = 0.20 ms and a range of drift tube temperatures, along with corresponding model predictions shown as solid lines. The scatter in the 325 °C data is the result of thermal noise in the width data. The fit between model and experiment is poorest at high temperature and high voltage. Measured resolving power values are higher than those predicted by the model, because the measured peak widths are narrower than expected. Because diffusion is quite unimportant in these peak widths, the phenomenon must be associated with a small negative temperature dependence in β or γ. This is another manifestation of the effect noted in the discussion of Figure 4 above.

Contributions of V, T, t_g, L, and K to Resolving Power. The effects of the various operating parameters on resolving power are apparent in eqs 12–14 and summarized for the diffusion-dominated and pulse-width-dominated regimes in Table 3.

In the diffusion-dominated low-voltage regime ($R_d \ll R_p$), resolving power is unaffected by an ion's mobility or the length of the drift tube. In this regime, one would simply operate at the highest voltage and lowest temperature possible to achieve the highest resolving power. As we have noted above, however, the weakness of the ion signals in the diffusion-dominated regime requires one to operate where diffusion and initial pulse make comparable contributions to peak width or in the pulse-width-dominated regime.

In the pulse-width-dominated regime ($R_p \ll R_d$), the increases of resolving power with V^{-1}, T^{-1}, L^2, and K^{-1} all arise through the increase of drift time with these parameters. Because IMS signal strength is essentially proportional to Vt_g, using either decreased V or t_g to increase resolving power necessitates striking some

balance between sensitivity and resolving power. Since K is, of course, a property of the ion of interest and not subject to change, only increasing drift tube length offers any possibility of increasing IMS resolving power without loss of signal strength. Our investigations with different tube lengths in this study clearly exhibit the enhancement of resolving power available with a longer tube. Brokenshire[8] has described a tube of 10 cm diameter and $L = 44$ cm, reporting resolving power 5–10 times that of an 8 cm instrument.

Because the dependence of resolving power on voltage changes from $V^{1/2}$ to V^{-1} as one moves from the diffusion-dominated to the pulse-width-dominated regime, resolving power is a maximum at a certain voltage, V_{opt}, an observation first made by Spangler and Collins.[2] Differentiating eq 12 with respect to voltage, setting the result equal to zero, and solving for V yields

$$V_{opt}\left(\frac{\alpha T L^4}{2(\gamma + \beta t_g^2)K^2}\right)^{1/3} \quad (15)$$

Aside from a missing cube root and their inclusion of the η parameter, this is equivalent to Spangler and Collins's eq 24.[2] Substituting eq 15 for V in eq 12 and solving for R yields an expression for the maximum resolving power possible for a particular drift tube and choice of operating conditions:

$$R_{max} = \left(\frac{L^2}{2.598(\gamma + \beta t_g^2)^{1/2}\alpha T K}\right)^{1/3} \quad (16)$$

Values of V_{opt} and R_{max} for the drift tubes used in this study are given in Table 2 for $T = 225$ °C, $t_g = 0.20$ ms, and $K = 4.25$ cm²/V s. On the basis of the $L^{2/3}$ dependence of R_{max}, we would expect Brokenshire's 44 cm instrument to have a maximum resolving power about 3.1 times that of a PCP instrument using the same pulse width and temperature.

One further quantity of interest for a drift tube is its maximum resolving power, expressed as a fraction of the resolving power obtainable with an "ideal" instrument of the same drift length (i.e., an instrument with $\alpha = 0.957 \times 10^{-3}$, $\beta = 1$, and $\gamma = 0$). Equation 16 quickly yields

$$\frac{R_{max}}{R_{ideal}} = \left(\frac{0.957 \times 10^{-3}}{\alpha\left(\frac{\gamma}{t_g^2} + \beta\right)^{1/2}}\right)^{1/3} \quad (17)$$

This ratio is also reported for the drift tubes used in this study in Table 2.

Factors Affecting α, β, and γ. All the measured α, β, and γ parameters in Table 2 exceed the "ideal" values predicted by eq 9, so that the diffusion, pulse width, and constant terms in eq 11 all make peaks wider than expected from the simplest theory.

The α term includes, in addition to actual diffusion, other diffusion-like processes, i.e., broadening processes which depend on the time ions spend in the drift tube. One effect of this sort would be additional diffusion due to ions having higher effective temperature than their surroundings, as in eq 10, from the extra energy being pumped into them by the drift field. However, as mentioned above, this effect is expected to be small for ions of the size studied with IMS.[6] In any event, all drift tubes will be affected about equally by this phenomenon, whatever its magnitude, so this process cannot account for differences observed between IMS instruments in this study.

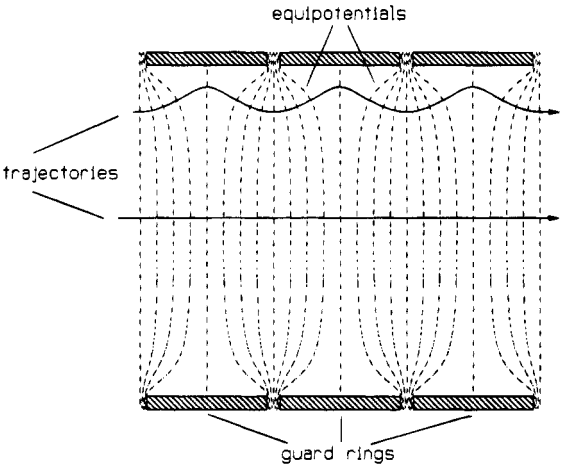

Figure 8. Equipotentials and ion trajectories in a segmented drift tube.

Another factor which can contribute to broadened peaks is radial variation in the electric field. For instruments constructed as stacks of wide rings, as are all the tubes in the present study, the drift field becomes progressively less homogeneous as one moves away from the tube axis, as shown schematically in Figure 8. The closer an ion's path is to the tube wall, the wider the oscillations in electric field it experiences. Any inhomogeneity in the electric field will cause a drift delay relative to an ion which experiences a perfectly uniform field. To see this, suppose that the drift space is divided into two regions of length $L/2$ and that the voltage drop across each region is uniform and equal to $V(1 + \epsilon)/2$ in the first region and $V(1 - \epsilon)/2$ in the second region. Thus the total voltage drop across the drift space is V, and the drift time t_d' of an ion will be equal to the sum of the drift times across the two regions,

$$t_d' = t_{d1} + t_{d2} = \frac{L^2}{KV(1 + \epsilon)(1 - \epsilon)} = \frac{1}{1 - \epsilon^2}t_d > t_d \quad (18)$$

where eq 2 has been used. Note that this same expression would hold for a drift tube divided into a larger number of alternating zones of higher and lower electric field. To accurately compute the effects of field inhomogeneity on drift time in a specific instrument, it would be necessary to map the electric field and to calculate line integrals for an array of ion trajectories. For our present purpose, we merely argue that the greater the inhomogeneity in the electric field, the longer the drift time. We also note that differences in drift time arising from variations in field homogeneity are probably responsible for much of the scatter in tabulated K_0 values.[9] The various IMS instruments used in this study also did not yield identical K_0 values. For example, tube A at 275 °C and tube D at 240 °C yielded 2.52 and 2.76 cm²/sV, respectively, for the K_0 of $(H_2O)_nH^+$.

If every ion experiences exactly the same inhomogeneous electric field, the drift time will be longer and the diffusion

(8) Brokenshire, J. L. FACSS Meeting, Anaheim, CA, October 1991.

(9) Shumate, C.; St. Louis, R. H.; Hill, H. H., Jr. *J. Chromatogr.* **1986**, *373*, 141–173.

contribution to peak width according to eq 8 will correspondingly increase compared to the homogeneous case, but α will be unaffected, since t_d' has exactly the same voltage dependence as t_d. It is differences between the electric fields experienced by different ions that lead to additional peak broadening. An ion pulse leaves the entrance gate as a thin, flat disk, but while in the drift region ions at the outer edge of the disk will lag behind those on the tube axis and lead to a broadened and possibly distorted peak at the collector. If ions in the center of the drift tube experience a homogeneous field while those at the edge of the ion disk find a field varying by about $\pm 1.4\epsilon$, the width due to homogeneity differences, w_{hom}, will be given roughly by

$$w_{hom} \cong t_d' - t_d = \frac{\epsilon^2}{1 - \epsilon^2} t_d \qquad (19)$$

Equation 19 is similar to eq 8 in that the width is proportional to the drift time, but different in that w_{hom} lacks the $(T/V)^{1/2}$ dependence of t_{diff}. If eq 9 were modified by the inclusion of the homogeneity effect, the model equation would become

$$w^2 = t_g^2 + \left[\frac{16 \ln 2k}{q} + \frac{\epsilon^4}{(1 - \epsilon^2)^2} \frac{V}{T}\right] \frac{T t_d^2}{V} \qquad (20)$$

A term like the second one in the square brackets could account for α values greater than ideal. The functional form indicates that plots of w^2 against Tt_d^2/V should be concave downward, with the slope increasing most notably at low values of Tt_d^2/V. Our plots, such as Figure 2, often seem to show such behavior, but the scatter in the data is such that a firm conclusion is difficult to reach.

The physical dimensions of the four drift tubes in this study tend to confirm these ideas about the effect of field inhomogeneity on peak width. Firstly, the ionization region, where all the primary and secondary ionization processes are presumed to occur, should have a diameter less than the drift region in order to produce a narrow beam of ions that will travel in the most homogeneous portion of the field close to the tube axis. Secondly, a large diameter drift region is desirable, both to increase the field homogeneity along the tube axis and to increase the diameter of the zone where the field is highly homogeneous. Tube C has a much smaller diameter than any of the others, and its much less uniform field presumably gives rise to its large observed α value. While tubes A and B have drift regions slightly greater in diameter than that of tube D, the latter has an ionization region only half as wide as those of A and B. Thus an ion pulse in tube D is more closely confined around the tube axis and should experience a more uniform field than a wider diameter pulse in tubes A or B. This could account for the larger α values for A and B. However, Spangler and Cohen's discussion[10] of electric field modeling by Albritton et al.[11] indicates that tubes A, B, and D should all have less than 1% variation in the electric field experienced by ions in the drift space. In contrast, equating the expression in square brackets in eq 20 with α values from Table 2 and values of V/T representing averages for conditions employed in the experiments with the three tubes, ϵ values of about 0.1 are computed for A, B, and D, indicating an electric field with much more than 1% variation.

Other than tube A, all the IMS instruments had similar values for the pulse width parameter (β = 1.13–1.24). The data of Spangler and Collins[2] are similar, yielding $\beta = 1.15$ when treated as in Figure 3. The ions at the edge of a pulse experience electrostatic repulsion due to all the same-charge ions within the pulse, thus producing broadening of the pulse. The repulsive electric field at the boundary of a pulse is proportional to the pulse duration t_g[2,7] and would lead to plots of w^2 against t_g^2 having slopes greater than 1 but remaining linear as in the ideal case. Tube A was found to have a construction flaw in its collector region which led to the presence of broad ghost peaks. These in turn confounded our method of measuring peak widths and resulted in an anomolously large β. In fact, it was the large β which originally made us realize the tube was flawed.

The γ parameter comes from broadening processes which remain after processes connected with pulse width and time of residence in the drift space have been removed. These could include amplifier rise time and collector response time. The amplifier rise time in all our experiments was 0.1 ms (10–90%), a value which would be consistent with the observed range of $\gamma^{1/2}$ = 0.07–0.15 ms. Also, the collector begins to respond to an ion cloud before it makes actual contact with the metal surface, in fact as soon as the cloud has passed a horizon in the vicinity of the aperture grid. Aperture grids are typically 0.5 mm away from the collector, so the flight time between grid and collector is on the order of 0.05 ms, large enough to possibly contribute to γ. However, we would also expect this time to be proportional to the drift voltage and thus to be eliminated in the diffusion extrapolation.

While there is thus some justification for associating the α, β, and γ parameters with physical conditions in the drift tube, these remain semiempirical values derived from fitting experimental data. Even with this loose connection to theory, however, the fitting process and the parameters still seem useful as measures of instrument performance and as tools for comparison and prediction.

ACKNOWLEDGMENT

The authors thank David Atkinson for gathering some of the peak width data. Portions of this work were presented at the 47th Northwest Regional Meeting of the American Chemical Society, Missoula, MT, June 17–19, 1992. The work was supported in part by NSF Grant CHE-9021094 to Gonzaga University.

Received for review April 8, 1994. Accepted August 24, 1994.[⊗]

[⊗] Abstract published in *Advance ACS Abstracts,* October 1, 1994.

(10) Spangler, G. E.; Cohen, M. J. In *Plasma Chromatography*; Carr, T. W., Ed.; Plenum Press: New York, 1984; p 6.

(11) Albritton, D. L.; Martin, D. W.; McDaniel, E. W.; Miller, T. M.; Moseley, J. T. *Measurement of the Low-Energy Transport Parameters of Mass-Identified Ions in Gases*, Appendix IV; Georgia Institute of Technology: Atlanta, 1967.